Hextuple-Inverter Configuration for Multilevel Nine-Phase Symmetrical Open-Winding Converter

Sanjeevi Kumar Padmanaban[1], Mahajan Sagar Bhaskar[2], Pandav Kiran Maroti[3],
Frede Blaabjerg[4], Pierluigi Siano[5] and Valentin Oleschuk[6]
[1]*Research & Development, Ohm Technologies, Chennai, India*
[2,3]*Dept. of Electrical & Electronics Engg., MIT, Aurangabad, India*
[4]*Center for Reliable Power Electronics (CORPE), Dept. of Energy Technology, Aalborg, University, Denmark*
[5]*Dept. of Industrial Engg., University of Salerno, Salerno, Italy*
[6]*Institute of Power Engg., Academy of Science of Moldova, Moldova*
E-mail: [1]sanjeevi_12@yahoo.co.in, [2]sagar25.mahajan@gmail.com, [3]kiranpandav88@yahoo.co.in,
[4]fbl@et.aau.dk, [5]psiano@unisa.it, [6]oleschukv@hotmail.com

***Abstract*—Hextuple-inverter configuration for multilevel nine-phase symmetrical open-winding DC converter is articulated in this work. Power modular unit consists of six classical three-phase voltage source inverters (VSI). Each VSI includes one bi-directional device (MOSFET/IGBT) per each phase and link to two capacitors for neutral connection. A modified single carrier five-level modulation (MSCFM) algorithm is developed and modulates each 2-level VSI as 5-level multilevel inverter (MLI). A set of test results is presented, which are observed from the model based developments in numerical simulation software's (Matlab/PLECS). The results always showed good conformity with the developed theoretical background under working conditions. The proposed converter found suited for (low-voltage/high current) electric vehicles, DC tractions and 'More-Electric Aircraft' applications.**

Keywords: ***Nine-phase Inverter, Symmetrical/ Asymmetrical Inverter, Hex-inverter, Multilevel Inverters, Multiphase Drives, Multiple Space Vectors, Pulse-width Modulation***

I. INTRODUCTION

Multiphase DC drives are the renowned technologies for reliable and fault tolerant, redundant with low-voltage and high-current configurations. Apart, benefit by reducing DC link ripple, increased power density, and reduced per-phase of the inverter rating (MOSFET/IGBT) [1-6]. Exploiting the above advantages, this article focused on nine-phase multilevel DC converter configuration for open-winding loads. Usually configured by any two adjacent winding phases are spatially displaced by 40^0 (symmetrical type) [1-2] or by 20^0 (asymmetrical) [1-2]. Advantages, easy to split the phase windings into classical three-phase windings pair and driven by multiple standard 2-level VSI as a multiphase converter [2-6]. Topologies are applicable to several low-voltage/high current, i.e. electric vehicles, DC traction and 'More-Electric Aircraft' (MEA) propulsion systems [7-8]. Recently multiphase DC drives replaced the mechanical, hydraulic and pneumatic actuators in MEA. Therefore, compact size, high reliability with fault tolerant capabilities and improved overall aeronautic propulsion performances [8]. Multilevel inverters (MLIs) had proved that they are the predominant to 2-level VSI counterparts for high voltage (HV) synthesis by the multiple DC sources [9]. Renowned benefits are the reduced total harmonic distortion (THD), and limited dv/dt in the output voltages with limited rating devices [9]. Several failures are still addressed for multilevel inverters, mainly by the power parts (31-37.9)% by the mechanism of IGBT devices for high power applications [10-11]. Also, vulnerability arises due to the capacitors and gate control techniques [10-11]. Both multi-phase and multi-level inverter combined configurations become the evident for obtaining high power with low-voltage/high-current rated devices [2-6]. Classical 2-level VSIs are still reasonable topology for reliability and easy to configure as multi-phase and multi-level converters by multiple proper arrangement of VSIs [3]. Dual inverters are the standard solutions such cases, the two-level standard 3-Φ VSI are connected on either side of the open-windings perform as multilevel converter [3-6]. Difference in leg potential constitute the output phase voltages as multilevel generator, when couple of VSIs modulated as 3-level. Dual inverters hold the benefit of standard MLIs and homo-polar currents are nullified by the PWM techniques or by isolating DC sources [3-6]. But restricted with output voltage levels, each leg is limited to three-levels. [2-6].

Inspired by facts, this article developed modified dual inverter topologies for multilevel nine-phase symmetrical converter for open-winding loads and shown in Fig. 1 [3-6, 12]. A modified single carrier five-level modulation (MSCFM) technique (independent modulation for each VSI) is framed and generates 5-level outputs for each VSI [12-15]. Converter modular structure consists of six 2-level classical three-phase voltage source inverters (VSIs H and L). Further, each VSI as one bi-directional (IGBT) switch per phase and link the neutral with two capacitors as additional inclusion to the circuit. Each VSI is connected at the ends of open-windings for ensuring

978-1-4673-8586-2/16/$31.00 ©2016 IEEE

5-level in each leg phases [12-15]. Further, the flexibility of the topology utilizes six isolated DC sources as in Fig. 1 (top) or two isolated DC sources as in Fig. 2 (bottom) depending on available different sources (PV, fuel cells etc.,). Naturally, both cases the homo-polar components are null as the DC sources are isolated and balanced condition is presumed. Moreover, the total power is shared among the DC sources and sextupling the power capabilities of each VSIs (H and L) and compromise the benefit of standard 5-level MLIs. Reliability is ensured under fault conditions one or two or three….VSIs failed, but still propagates with available VSIs with degraded power ratings [3-6, 11]. To verify the performances, the proposed hex-inverter based multilevel nine-phase symmetrical open-winding converter is numerically modeled and tested with Matlab/PLECS simulation software's. Set of observed results is presented in this paper under balanced working conditions and shown good conformity with theoretical predictions.

II. Split-phase Decomposition Space Vector Transformation for Nine-Phase System

A nine-phase system can be represented by means of multiple space vectors (stationary references) as [2, 16]:

$$\overline{x}_1 = \frac{2}{9}\left[\begin{array}{l} x_1 + x_2\alpha^3 + x_3\alpha^6 + x_4\alpha + \\ x_5\alpha^4 + x_6\alpha^7 + x_7\alpha^2 + x_8\alpha^5 + x_9\alpha^8 \end{array}\right]$$

$$\overline{x}_2 = \frac{2}{9}\left[\begin{array}{l} x_1 + x_2\alpha^6 + x_3\alpha^3 + x_4\alpha^2 + \\ x_5\alpha^8 + x_6\alpha^5 + x_7\alpha^4 + x_8\alpha^{10} + x_9\alpha^7 \end{array}\right]$$

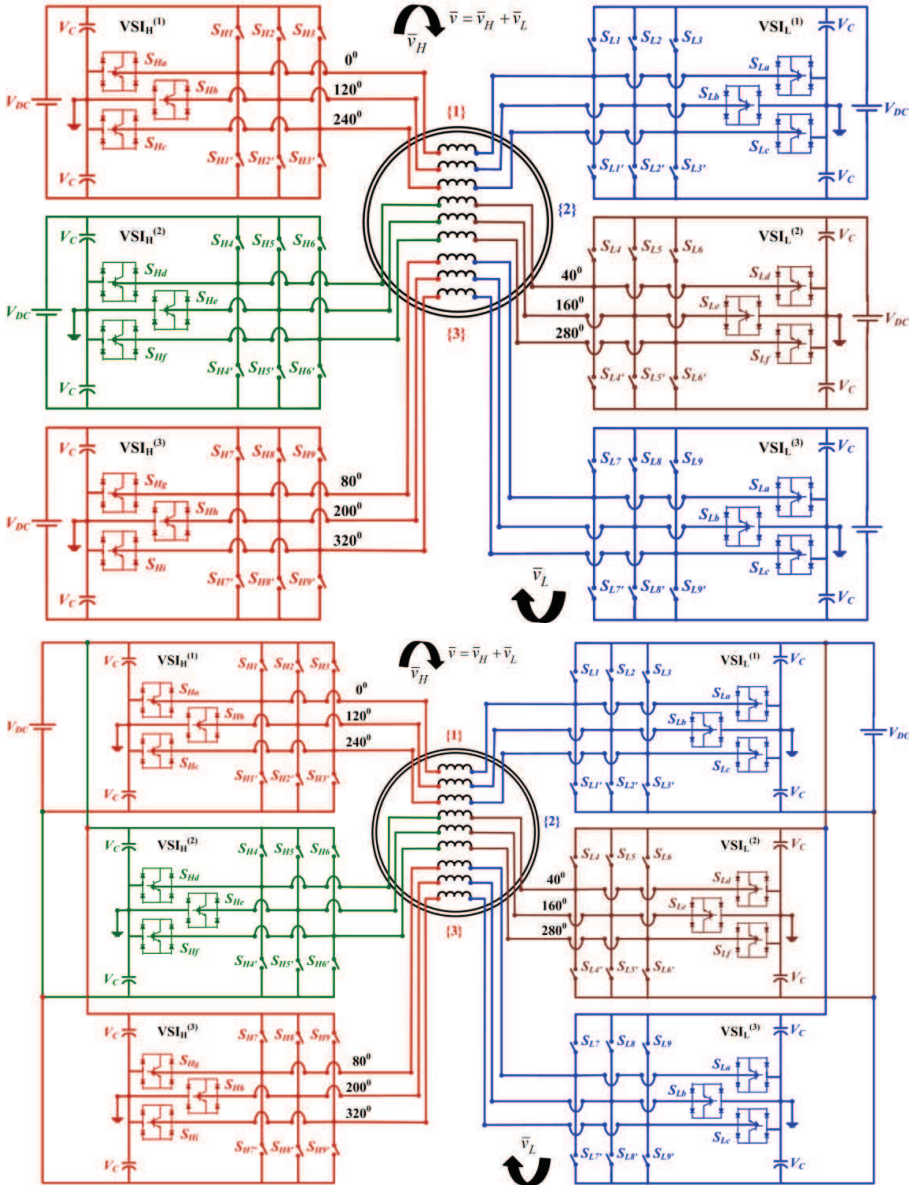

Fig. 1: Structure of Proposed Multilevel Nine-phase Open-winding Converter for Low-voltage/ High-current Applications, Top: Hex-inverter Isolated DC Sources, Bottom: Two Isolated Inverter DC Sources Configuration Systems

978-1-4673-8586-2/16/$31.00 ©2016 IEEE

$$\bar{x}_3 = \frac{2}{9}\left[\begin{array}{l} x_1 + x_2\alpha^3 + x_3\alpha^6 + x_4\alpha^3 + \\ x_5\alpha^6 + x_6\alpha^9 + x_7\alpha^6 + x_8\alpha^9 + x_9\alpha^{12} \end{array}\right]$$

$$\bar{x}_4 = \frac{2}{9}\left[\begin{array}{l} x_1 + x_2\alpha^3 + x_3\alpha^6 + x_4\alpha^4 + \\ x_5\alpha^7 + x_6\alpha^{10} + x_7\alpha^8 + x_8\alpha^{11} + x_9\alpha^{14} \end{array}\right]$$

$$\bar{x}_0 = \frac{1}{9}\left[\begin{array}{l} \left(x_1 + x_2 + x_3\right) + \left(x_4 + x_5 + x_6\right) + \\ \left(x_7 + x_8 + x_9\right) \end{array}\right] \quad (1)$$

To be noted, where, $\alpha = exp\ (j2\pi/9)$, symmetrical converters spatial displacement between adjacent windings [1-2]. The multiple space vectors $\bar{x}_1, \bar{x}_2, \bar{x}_4$ are the three rotating vectors and $x_0, \bar{x}_3$ are the zero sequence components. Four multiple space vectors are exposed in the sub-spaces of d_1-q_1, d_2-q_2, d_3-q_3, and d_4-q_4 respectively. To introduce the split-phase space vector decomposition transformation to six VSI fed nine-phase open-windings supplied by six/two isolated DC sources. The nine-phase system can be split into three three-phase sub-systems {1}, {2}, {3} as [2-6]:

$$\{1\}\begin{cases} x_1^{(1)} = x_1 \\ x_2^{(1)} = x_2 \\ x_3^{(1)} = x_3 \end{cases};\ \{2\}\begin{cases} x_1^{(2)} = x_4 \\ x_2^{(2)} = x_5 \\ x_3^{(2)} = x_6 \end{cases};\ \{3\}\begin{cases} x_1^{(3)} = x_7 \\ x_2^{(3)} = x_8 \\ x_3^{(3)} = x_9 \end{cases}. \quad (2)$$

The rotating three-phase space vectors $\bar{x}^{(1)}$, $\bar{x}^{(2)}$, $\bar{x}^{(3)}$ and corresponding zero-sequence components $x_0^{(1)}$, $x_0^{(2)}$, $x_0^{(3)}$ are defined for three three-phase sub-system {1}, {2}, {3} as:

$$\{1\}\begin{cases} \bar{x}^{(1)} = \frac{2}{3}\left[x_1^{(1)} + x_2^{(1)}\alpha^3 + x_3^{(1)}\alpha^6\right] \\ x_0^{(1)} = \frac{1}{3}\left[x_1^{(1)} + x_2^{(1)} + x_3^{(1)}\right] \end{cases}$$

$$\{2\}\begin{cases} \bar{x}^{(2)} = \frac{2}{3}\left[x_1^{(2)} + x_2^{(2)}\alpha^3 + x_3^{(2)}\alpha^6\right] \\ x_0^{(2)} = \frac{1}{3}\left[x_1^{(2)} + x_2^{(2)} + x_3^{(2)}\right] \end{cases}$$

$$\{3\}\begin{cases} \bar{x}^{(3)} = \frac{2}{3}\left[x_1^{(3)} + x_2^{(3)}\alpha^3 + x_3^{(3)}\alpha^6\right] \\ x_0^{(3)} = \frac{1}{3}\left[x_1^{(3)} + x_2^{(3)} + x_3^{(3)}\right] \end{cases} \quad (3)$$

Multiple space vectors and split-phase (three-phase) space vectors is related by substituting (3) and (2) in (1) and emphasized as:

$$x_0 = \frac{1}{3}\left[x_0^{(1)} + x_0^{(2)} + x_0^{(3)}\right]$$

$$\bar{x}_1 = \frac{1}{3}\left[\bar{x}^{(1)} + \alpha\ \bar{x}^{(2)} + \alpha^2\bar{x}^{(3)}\right]$$

$$\bar{x}_2^* = \frac{1}{3}\left[\bar{x}^{(1)} + \alpha^{-2}\ \bar{x}^{(2)} + \alpha^{-4}\bar{x}^{(3)}\right]$$

$$\bar{x}_3 = \frac{2}{3}\left[x_0^{(1)} + \alpha^3 x_0^{(2)} + \alpha^6 x_0^{(3)}\right]$$

$$\bar{x}_4 = \frac{1}{3}\left[\bar{x}^{(1)} + \alpha^4\ \bar{x}^{(2)} + \alpha^8\bar{x}^{(3)}\right] \quad (4)$$

Inverse transformation to (4) is given by:

$$\{1\}\rightarrow\begin{cases} \bar{x}^{(1)} = \bar{x}_1 + \bar{x}_2^* + \bar{x}_4 \\ x_0^{(1)} = \bar{x}_1 + \bar{x}_3 \end{cases};\ \{2\}\rightarrow\begin{cases} \bar{x}^{(2)} = \alpha^{-1}\bar{x}_1 + \alpha^2\bar{x}_2^* + \alpha^4\bar{x}_4 \\ x_0^{(2)} = \bar{x}_1 + \alpha^3\bar{x}_3 \end{cases};$$

$$\{3\}\rightarrow\begin{cases} \bar{x}^{(3)} = \alpha^{-2}\bar{x}_1 + \alpha^4\bar{x}_2^* + \alpha^8\bar{x}_4 \\ x_0^{(3)} = \bar{x}_1 + \alpha^6\bar{x}_3 \end{cases} \quad (5)$$

Noted, where the symbols "*" denotes complex conjugate, respectively.

Hexuple-Inverter Single Carrier based Five-Level Modulation Algorithm

The P total electric power of the multilevel nine-phase converter can expressed as the sum of the power of the three three-phase windings {1}, {2}, and {3} ($VSI_H^{(1)}$, $VSI_L^{(1)}$, $VSI_H^{(2)}$, $VSI_L^{(2)}$, and $VSI_H^{(3)}$, $VSI_L^{(3)}$) [2-6, 12-16]:

$$P = P^{(1)} + P^{(2)} + P^{(3)}$$

$$P = \frac{3}{2}\bar{v}^{(1)} \cdot \bar{i}^{(1)} + \frac{3}{2}\bar{v}^{(2)} \cdot \bar{i}^{(2)} + \frac{3}{2}\bar{v}^{(3)} \cdot \bar{i}^{(3)} \quad (6)$$

If the bi-directional switch per phases and two capacitors with neutral point are neglected in the Fig. 1 (top and bottom), results in three standard two-level inverters. Now, the modulations can be performed as standard VSIs. By application of space vector theory, the output voltage vector $\bar{v}$ of the nine-phase inverter can be expressed as the sum of the voltage vectors of three three-phase windings {1}-$\bar{v}^{(1)}$, {2}-$\bar{v}^{(2)}$, and {3}-$\bar{v}^{(3)}$ by the six three-phase inverters ($VSI_H^{(1)}$, $VSI_L^{(1)}$, $VSI_H^{(2)}$, $VSI_L^{(2)}$, and $VSI_H^{(3)}$, $VSI_L^{(3)}$) and given as [3]:

$$\bar{v} = \bar{v}^{(1)} + \bar{v}^{(2)} + \bar{v}^{(3)} \quad (7)$$

By splitting nine-phase windings into standard three three-phase windings then (7) by considering (3) then the modulating vectors can represent for first-, second-, and third- three-phase windings as below:

$$\bar{v}^{(1)} = \bar{v}_H^{(1)} + \bar{v}_L^{(1)} \quad (8)$$

$$\bar{v}^{(2)} = \bar{v}_H^{(2)} + \bar{v}_L^{(2)} \quad (9)$$

$$\bar{v}^{(3)} = \bar{v}_H^{(3)} + \bar{v}_L^{(3)} \quad (10)$$

Now, considering (3), then (8) to (10) for inverters $VSI_H^{(1)}$, $VSI_L^{(1)}$, $VSI_H^{(2)}$, $VSI_L^{(2)}$, $VSI_H^{(3)}$, and $VSI_L^{(3)}$, then the modulating vectors can be expressed as:

$$\begin{aligned} \bar{v}_H^{(1)} &= \tfrac{1}{3}V_{DC}\left(S_{H1} + S_{H2}e^{j2\pi/3} + S_{H3}e^{j4\pi/3}\right) \\ \bar{v}_L^{(1)} &= -\tfrac{1}{3}V_{DC}\left(S_{L1} + S_{L2}e^{j2\pi/3} + S_{L3}e^{j4\pi/3}\right) \end{aligned} \quad (11)$$

$$\begin{aligned} \bar{v}_H^{(2)} &= \tfrac{1}{3}V_{DC}\left(S_{H4}\alpha + S_{H5}\alpha e^{j2\pi/3} + S_{H6}\alpha e^{j4\pi/3}\right) \\ \bar{v}_L^{(2)} &= -\tfrac{1}{3}V_{DC}\left(S_{L4}\alpha + S_{L5}\alpha e^{j2\pi/3} + S_{L6}\alpha e^{j4\pi/3}\right) \end{aligned} \quad (12)$$

978-1-4673-8586-2/16/$31.00 ©2016 IEEE

$$\bar{v}_H^{(3)} = \tfrac{1}{3}V_{DC}\left(S_{H7}\alpha^2 + S_{H8}\alpha^2 e^{j2\pi/3} + S_{H9}\alpha^2 e^{j4\pi/3}\right)$$
$$\bar{v}_L^{(3)} = -\tfrac{1}{3}V_{DC}\left(S_{L7}\alpha^2 + S_{L8}\alpha^2 e^{j2\pi/3} + S_{L9}\alpha^2 e^{j4\pi/3}\right) \quad (13)$$

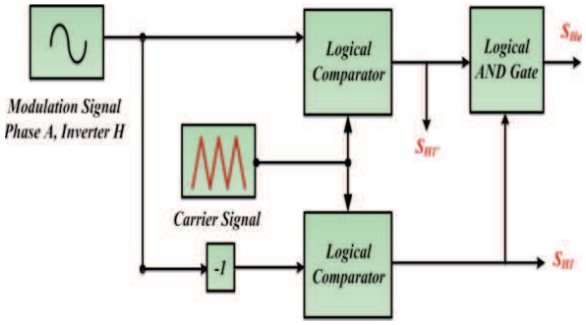

Fig. 2: Single Carrier Multilevel PWM Algorithm for Phase 'a' of Inverter $VSI_H^{(1)}$

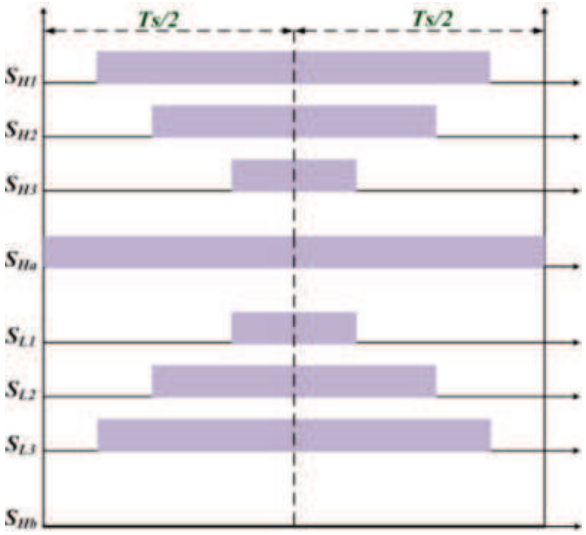

Fig. 3: PWM Pattern of Inverters $VSI_H^{(1)}$ (Top-three) and $VSI_L^{(1)}$ (Bottom-three) Modulation Index = 0.8)

Substitute (11) to (14), the (7) the modulating vector of nine-phase windings can be expressed as:

$$\bar{v} = \tfrac{1}{3}V_{DC}\begin{pmatrix} S_{H1}+S_{H2}e^{j2\pi/3}+S_{H3}e^{j4\pi/3}- \\ S_{L1}+S_{L2}e^{j2\pi/3}+S_{L3}e^{j4\pi/3}+ \\ S_{H4}\alpha+S_{H5}\alpha e^{j2\pi/3}+S_{H6}\alpha e^{j4\pi/3}- \\ S_{L4}\alpha+S_{L5}\alpha e^{j2\pi/3}+S_{L6}\alpha e^{j4\pi/3}+ \\ S_{H7}\alpha^2+S_{H8}\alpha^2 e^{j2\pi/3}+S_{H9}\alpha^2 e^{j4\pi/3}- \\ S_{L7}\alpha^2+S_{L8}\alpha^2 e^{j2\pi/3}+S_{L9}\alpha^2 e^{j4\pi/3} \end{pmatrix} \quad (14)$$

Therefore, now the arbitrary modulating vector for the nine-phase inverter can be determined by the information of nine VSI [2-6]:

For single, dual three-phase VSI ($VSI_H^{(1)}$ and $VSI_L^{(1)}$), the switching logic, upper-states are $\{S_H, S_{H1}, S_{H2}, S_{H3}\}$, lower-states are $\{S_L, S_{L1}, S_{L2}, S_{L3}\} = \{1, 0\}$. Assumed homo-polar components are null, therefore, is balanced conditions, then (16) can be split as six separate three-phase VSI. For simplified investigation, the analyses are performed based on single carrier based 5-level modulation technique [12-14]. The modulating reference signals are exposed to standard triangular carrier for utilizing maximum DC buses and to generate 5-level output operation.

The single carrier (MSCFM) modulation algorithm for $VSI_H^{(1)}$, and $VSI_L^{(1)}$ to generate 5-level across the leg-phase 'a' is shown in Fig. 2. Noted, the same logic applied to all other leg-phases (b, c, d, e, f, g, h, i) of VSIs ($VSI_H^{(2)}$, $VSI_L^{(2)}$, $VSI_H^{(3)}$, $VSI_L^{(3)}$), and to keep the proper phase-shift between the reference modulating signals as $\alpha = exp\ (j2\pi/9)$. Phase 'a', switch S_{Ha} and S_{La} modulated throughout the fundamental cycle, i.e. swaps {1, 0} with switching period. Switch S_{H1} modulated first-half as ON and retains OFF second half of the fundamental period. While the switch S_{L1} modulated first-half as OFF and retains ON second-half of the fundamental period. Noted, the same strategy is applied to other phases (b, c, d, e, f, g, h, i) to generate a five-level outputs. Fig. 3 shows the switching pattern of the 5-level modulation for inverters $VSI_H^{(1)}$ and $VSI_L^{(1)}$ with the modulation index of 0.8.

III. Numerically Observed Results and Discussion

Effectiveness of the proposed multilevel nine-phase symmetrical converter is tested using numerical modeled in Matlab/PLECS simulation software's. Table I gives the detailed parameters taken for investigation under balanced conditions. Modulation index of six $VSI_H^{(1)}$, $VSI_L^{(1)}$, $VSI_H^{(2)}$, $VSI_L^{(2)}$, $VSI_H^{(3)}$, $VSI_L^{(3)}$ kept 0.8 and therefore, overall modulation index of nine-phase converter is 0.8. Fig. 4 and Fig. 5 elaborate the observed numerical simulation behavior of the converter system under test.

TABLE 1: Main Parameters of Nine-Phase Multilevel Converter

DC Bus	*VDC*	= 200V
Load Resistances	*R*	= 8 Ω
Load Inductances	*L*	= 10mH
Fundamental Frequency	*F*	= 50Hz
Switching Frequency	*FS*	= 5 KHz
Capacitors	*VC*	= 2200μF

Fig. 4(A), Fig. 4(B), Fig. 4(C), Fig. 4(D), Fig. 4(E) and Fig. 4(F) shows the generated line-line voltages of inverters $VSI_H^{(1)}$, $VSI_L^{(1)}$, $VSI_H^{(2)}$, $VSI_L^{(2)}$, $VSI_H^{(3)}$, $VSI_L^{(3)}$, of first {1}, second {2}, third {3}, three-phase windings. Also, depicted with their corresponding fundamental components the same Figures. First, it is observed that fundamental components are equal in amplitude and proven balanced operation. Second, 40^0 spatial phase displacement between VSIs of first {1}, second {2} and third {3} three-phase open-windings are observed and it was expected. Third, the voltages generated by each couple of VSI_H and VSI_L are out of phase with respect to the other. Fourth, the results confirm that each single VSI (H and L) generated 5-level output voltages by the developed MSCFM PWM technique. It is concluded that

proposed converter overcomes the drawback of limited voltage levels of addressing dual inverter configurations [2-6].

Figure 4(G), Fig. 4(H), Fig. 4(I), Fig. 4(J), Fig. 4(K) and Fig. 4(L) are the artificially calculated first-phase voltages of inverters $VSI_H^{(1)}$, $VSI_L^{(1)}$, $VSI_H^{(2)}$, $VSI_L^{(2)}$, $VSI_H^{(3)}$, $VSI_L^{(3)}$, of first {1}, second {2}, third {3}, three-phase windings. Also, corresponding fundamental components are depicted in the same Figures and are in agreement with (11), (12) and (13). As expected, first it is observed that phase voltages of the VSIs (H and L) are 7-levels waveforms. Second fundamental components are equal with the same amplitude and the balanced, smooth operation is verified with modulation index = 0.8 for each VSI. Third, it could be confirmed that phase voltages generated by each couple of VSI_H and VSI_L are out of phase with respect to the other. Fourth, 40^0 spatial phase displacement between VSIs of first {1}, second {2} and third {3} three-phase open-windings are observed and as expected.

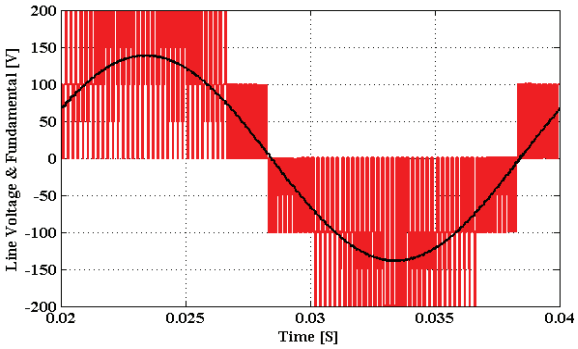

(A). Line–line Voltage of Inverter $VSI_H^{(1)}$

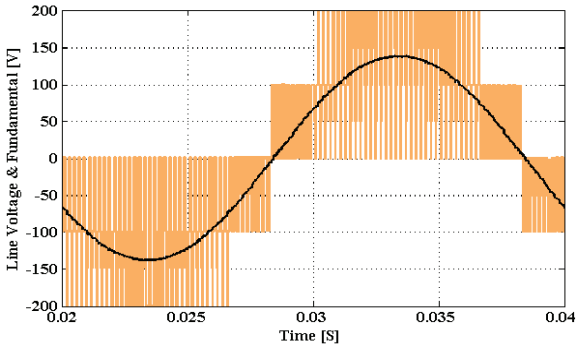

(B). Line–line Voltage of Inverter $VSI_L^{(1)}$

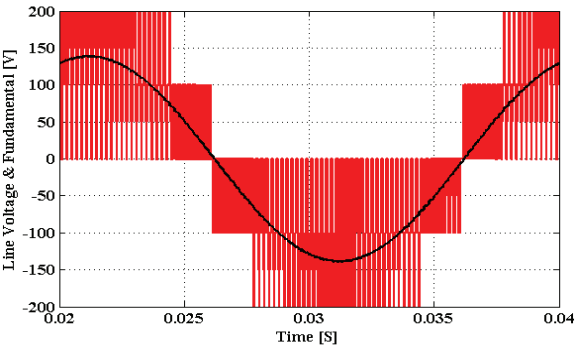

(C). Line–line Voltage of Inverter $VSI_H^{(2)}$

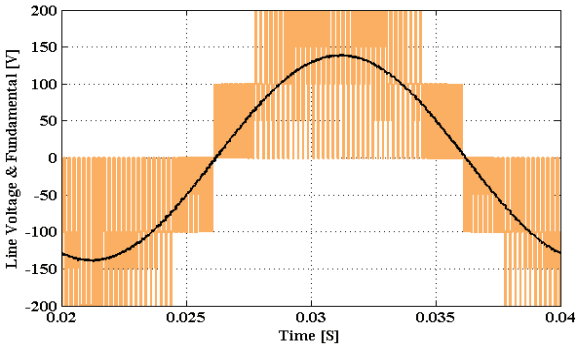

(D). Line–line Voltage of Inverter $VSI_L^{(2)}$

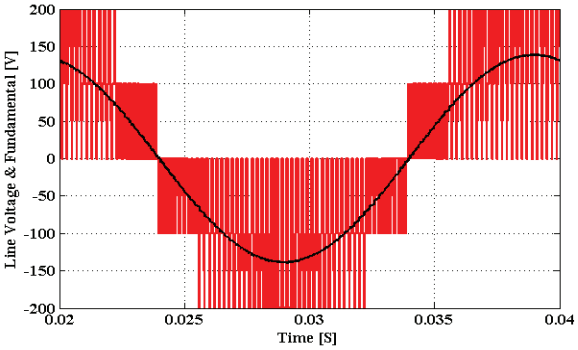

(E). Line–line Voltage of Inverter $VSI_H^{(3)}$

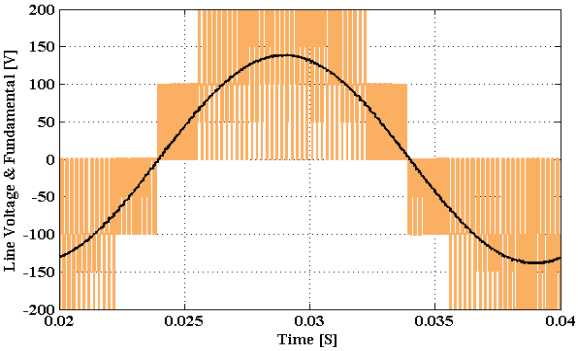

(F). Line–line Voltage of Inverter $VSI_L^{(3)}$

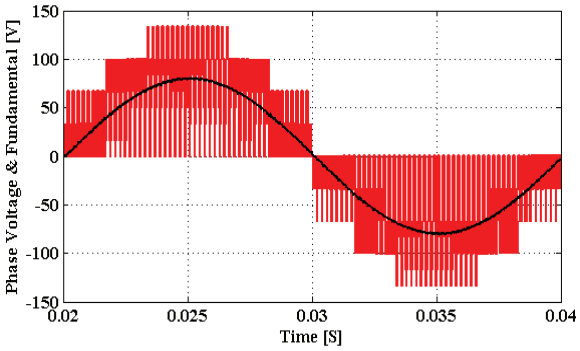

(G). Artificially Measured First-phase Voltage of Inverters $VSI_H^{(1)}$

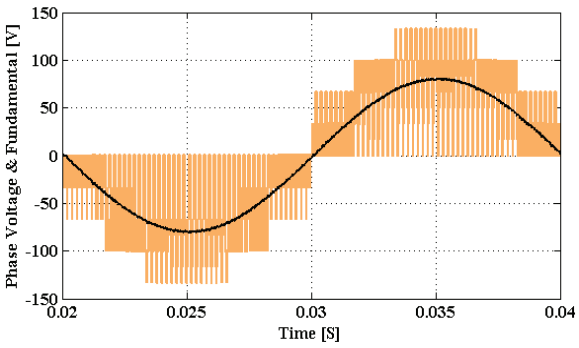

(H). Artificially Measured First-phase Voltage of Inverters $VSI_L^{(1)}$

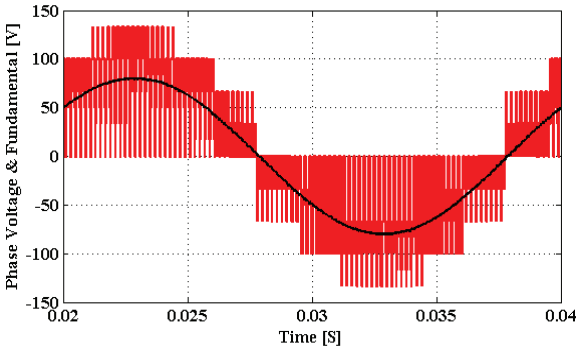

(I). Artificially Measured First-phase Voltage of Inverters $VSI_H^{(2)}$

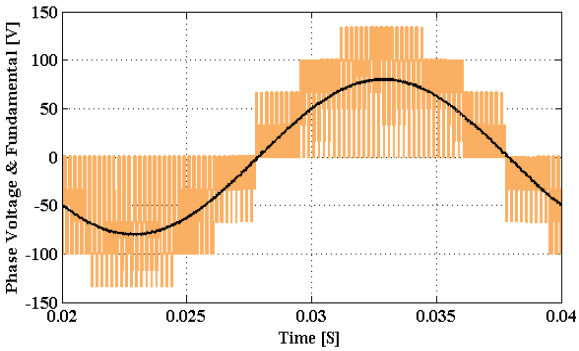

(J). Artificially Measured First-phase Voltage of Inverters $VSI_L^{(2)}$

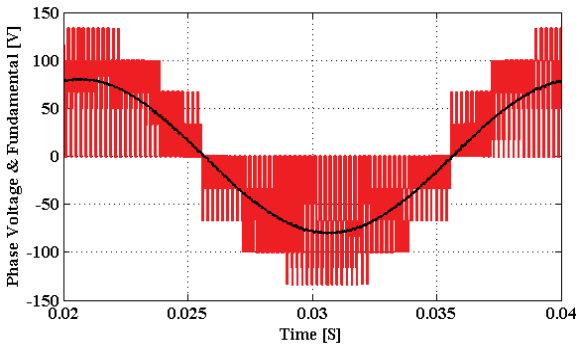

(K). Artificially Measured First-phase Voltage of Inverters $VSI_H^{(3)}$

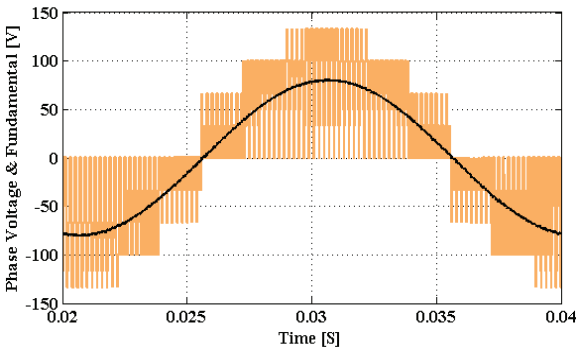

(L). Artificially Measured First-phase Voltage of Inverters $VSI_L^{(3)}$

Fig. 4: Observed Simulation Behavior of the Proposed Symmetrical Nine-phase Open-winding Converter. Modulation Index = 0.8, Kept for Balanced Operation. Voltages are Depicted with its Corresponding Fundamental Components, Left: Line-line Voltages, Right: Artificially Measured Phase Voltages of the VSIs (H and L)

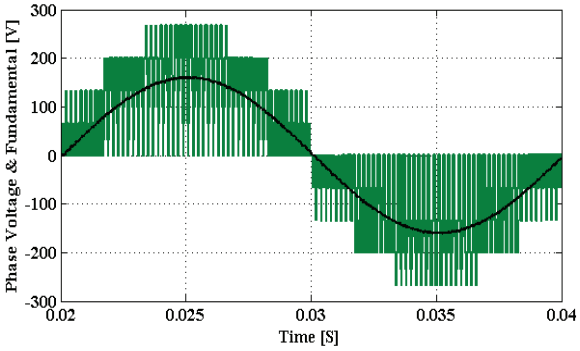

(A). First-phase Voltage ($VSI_H^{(1)}$ and $VSI_L^{(1)}$) of the First Open-winding {1}

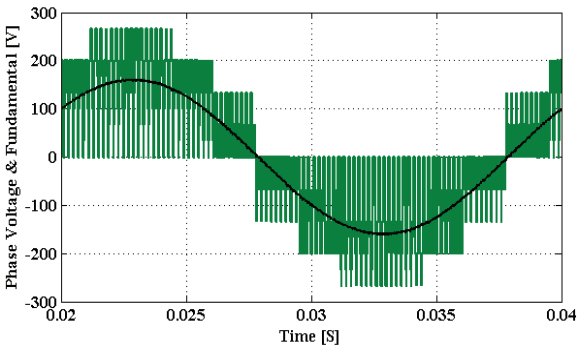

(B). First-phase Voltage ($VSI_H^{(2)}$ and $VSI_L^{(2)}$) of the Second Open-Winding {2}

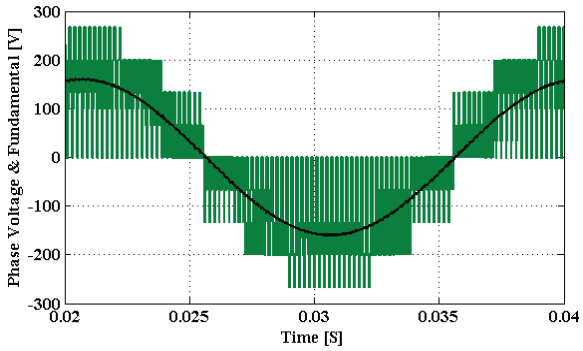

(C). First-phase Voltage ($VSI_H^{(3)}$ and $VSI_L^{(3)}$) of the Third Open-winding {3}

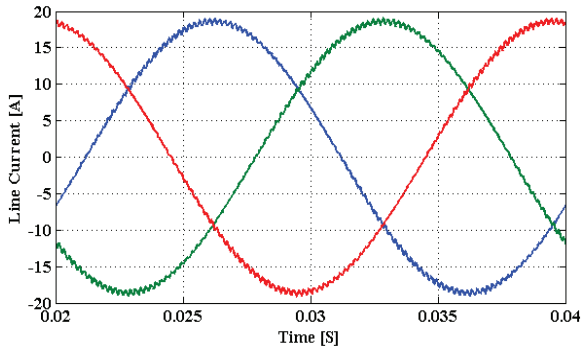

(D). First Three-phase Currents of the Open-windings {1}

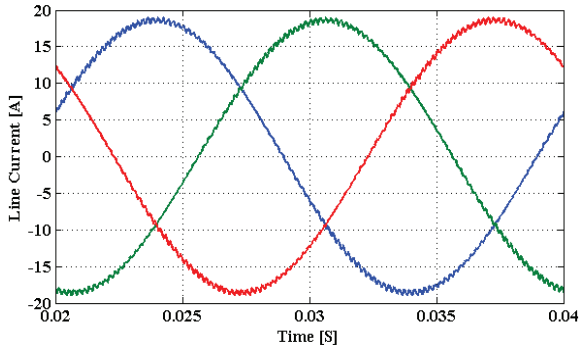

(E). Second Three-phase Currents of the Open-windings {2}

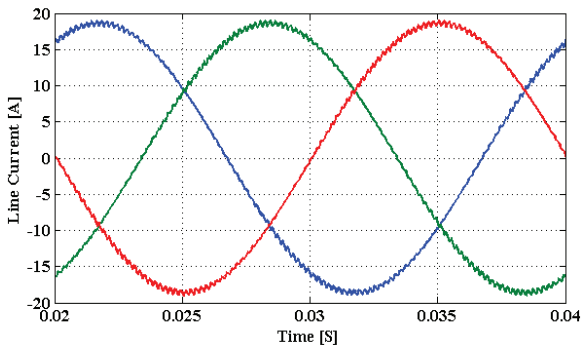

(F). Third Three-phase Currents of the Open-windings {3}

Fig. 5: Observed Simulation Behavior of the Proposed Symmetrical Nine-phase Open-winding Converter. Modulation Index = 0.8, Kept for Balanced Operation. Voltages are Depicted with its Corresponding Fundamental Components, Left: Open-windings Phase Voltages, Right: Nine-phase Open-Winding Currents

Figure 5(A), Fig. 5(B), Fig. 5(C) are the phase voltages generates by the first three-phase (phase 'a') {1}, second three-phase (phase'd') {2}, third three-phase (phase 'g') of the open-windings. Also, here time scaled average fundamental component are depicted in the same figures. First, the phase voltages generated are 7-levels in all three sets of open-windings {1}, {2} and {3}, as predicted the same. Second, obtained fundamental amplitude are the vector addition of phase voltages of inverters ($VSI_H^{(1)}$, $VSI_L^{(1)}$), ($VSI_H^{(2)}$, $VSI_L^{(2)}$) and ($VSI_H^{(3)}$, $VSI_L^{(3)}$) and shown agreement with (8), (9) and (10). Further, the overall modulation index of nine-phase converter is predicted and with agreement with the developed theoretical (14). Third, the depicted fundamental components shown that, the phase voltages are equal with the same amplitude and balanced operation with modulation index = 0.8 for each VSI is confirmed. Fourth, 40^0 spatial phase displacement is observed between phase voltages of open-windings {1}, {2} and {3} generated by VSIs ($VSI_H^{(1)}$, $VSI_L^{(1)}$), ($VSI_H^{(2)}$, $VSI_L^{(2)}$) and ($VSI_H^{(3)}$, $VSI_L^{(3)}$) and as expected the same. Hence, it is verified that all line-line and phase voltages generated by the VSIs confirm the requirement sets for nine-phase converter and shown good theoretical agreement with developed (8) to (14).

Correspondingly nine-phase currents, first three-phase {1}, second three-phase {2}, and third three-phase open-winding are shown in Fig. 5(D), Fig. 5(E) and Fig. 5(F) respectively. First, it is observed that currents are sinusoidal in nature and confirms the each VSI are modulated sinusoidally with developed MSCFM PWM technique. Second, spatial phase displacement of 40^0 is clearly noticed between the first three-phase {1}, second three-phase {2} and third three-phase {3} open-winding currents. Third, all nine-phase currents are equal with the same amplitude and shown balanced operation with set modulation index factor 0.8 and maintained throughout the propagation period. All presented results shown good agreement with set theoretical developments for open-windings converter. Finally, a nine-phase system can be investigated as three-phase systems and fed by multiple VSI as multi-phase/multi-level converter as prominent solution.

IV. Conclusion

This paper presented hex-inverter configuration for nine-phase symmetrical open-winding multilevel converter. Further, modified single carrier five-level modulation (MSCFM) algorithm was framed and modulates each VSI as equivalent to 5-level multilevel

978-1-4673-8586-2/16/$31.00 ©2016 IEEE

inverter. Confirmatory results are obtained by numerical simulation software's modeling are presented and discussed. Moreover, the total electric power was sextupling among the isolated DC sources of VSIs. Proposed DC converter effective for multiple batteries/fuel-cells fed system, where asymmetrical condition can be balanced. Fit for low-voltage/high-current application such as electrical vehicles, DC tractions and 'More-Electric Aircraft' (MEA) systems.

The investigation is still kept under study to develop optimized multilevel (5-level, limited *dv/dt*) PWM based on the carrier based or space vector modulation techniques for near future works.

REFERENCES

[1] E.Levi, R. Bojoi, F. Profumo, H.A. Toliyat, S. Williamson, "Multi¬phase induction motor drives–a technology status review, " IET Electr. Power Appl., vol. 1, no.4, pp. 489–516, July 2007.

[2] G.Grandi, G.Serra, A.Tani, "Space vector modulation of nine-phase voltage source inverters based on three-phase decomposition", Conf. Proc. IEEE European Conf. on Power Electron. and Appl., IEEE-EPE'07, Aalborg (Denmark), pp. 1–12, 2–5 Sept. 2007.

[3] P.Sanjeevikumar, G.Grandi, F.Blaabjerg, Patrick Wheeler, Olorunfemi Ojo, "Analysis and Implementation of Power Management and Control Strategy for Six-Phase Multilevel AC Drive System in Fault Condition", Engg. Science and Tech; An Intl. J. (JESTECH), Elsevier Pub., 13 Jul. 2015. Doi: 10.1016/j.jestch. 2015.07.007.

[4] G. Grandi, P. Sanjeevikumar, D. Ostojic, C. Rossi, "Quad-inverter configuration for multi-phase multi-level ac motor drives", Conf. Proc., Intl. Conf. Computational Technologies in Elect. and Electron. Engg., IEEE–SIBIRCON'10, Irkutsk Listvyanka (Russia), pp. 631–638, 11–15 Jul. 2010.

[5] P.Sanjeevikumar, G.Grandi, F.Blaabjerg, Joseph Olorunfemi Ojo, Patrick Wheeler, "Power Sharing Algorithm for Vector Controlled Six-Phase AC Motor with Four Customary Three-Phase Voltage Source Inverter Drive", Engg. Science and Tech; An Intl. J. (JESTECH), Elsevier Pub., vol. 16, no. 3, pp. 405–415, 11 Feb. 2015.

[6] G. Grandi, P. Sanjeevikumar, Y. Gritli, F. Filippetti, "Experimental investigation of fault-tolerant control strategies for quad-inverter converters", Conf. Proc. IEEE Intl. Conf. on Electrical System for Aircraft, Railway and Ship Propulsion, IEEE-ESARS'12, Bologna (Italy), pp. 1–8, 16–18 Oct. 2012.

[7] W. Cao, B.C. Mecrow, G.J. Atkinson, J.W. Bennett, D.J. Atkinson, "Overview of electric motor technologies used for More-Electric Aircraft (MEA)", IEEE Trans. on Ind. Electron., vol. 59, no. 9, pp. 3523–3531, Sept. 2012.

[8] F. Scuiller, J.F. Charpentier, E. Semail, "Multi-star multi-phase winding for a high power naval propulsion machine with low ripple torques and high fault tolerant ability, " Proc. of Vehicle Power and Propulsion Conference, Lille, France, pp. 1–5, 1–3 Sept. 2010.

[9] L. G. Franquelo, J. Rodriguez, J. I. Leon, S. Kouro, R. Portillo and M. M. Prats, "The age of multilevel converters arrives, " IEEE Ind. Electron. Magazine, vol. 2, no. 2, pp. 28–39, June 2008.

[10] S. Yang, A. Bryant, P. Mawby, D. Xiang, Li Ran, P. Tavner, "An industry-based survey of reliability in power electronic converters, " IEEE Trans. on Ind. Electron., vol. 47, no. 3, pp. 1441–1451, May–June 2011.

[11] Frede Blaabjerg, M.M.Pecht, "Robust Design and Reliability of Power Electronics", IEEE Trans. on Power Electron., vol. 30, no. 5, pp. 2373–2374, 2015.

[12] P.Sanjeevikumar, F.Blaabjerg, Patrick Wheeler, Olorunfemi Ojo, "Three-phase multilevel inverter configuration for open-winding high power application", Conf. Proc., The 6th IEEE Intl. Symp. on Power Electron. for Distributed Generation Systems, IEEE-PEDG'15, Aachen (Germany), 22–25 June 2015.

[13] P.Sanjeevikumar, F.Blaabjerg, Patrick Wheeler, Olorunfemi Ojo, Pandav K. Maroti, "A Novel Double Quad-Inverter Configuration for Multilevel Twelve-Phase Open- Winding Converter", Conf. Proc. of 7th IEEE Intl. Conf. on Power System, IEEE-ICPS'16, Indian Institute of Technology (IIT-Delhi), Delhi (India), 4–6 Mar. 2016.

[14] P.Sanjeevikumar, F.Blaabjerg, Patrick Wheeler, Raghav Khanna, S.B. Mahajan, Sanjeet Dwivedi, "Optimized Carrier Based Five-Level Generated Modified Dual Three-Phase Open- Winding Inverter For Medium Power Application", Conf. Prof. of IEEE International Transportation Electrification Conf. and Expo, Asia-Pacific, (IEEE-ITEC'16), Busan (Korea). 1–4 Jun. 2016.

[15] P.Sanjeevikumar, F.Blaabjerg, Patrick Wheeler, Kyo-Beum Lee, S.B. Mahajan, Sanjeet Dwivedi, "Five-Phase Five-Level Open-Winding/Star-Winding Inverter Drive For Low-Voltage/ High-Current Applications", Conf. Prof. of IEEE International Transportation Electrification Conf. and Expo, Asia-Pacific, (IEEE-ITEC'16), Busan (Korea). 1–4 Jun. 2016.

[16] P.Sanjeevikumar, M, Hontz, RKhanna, Patrick Wheeler, F. Blaabjerg, OlOjo, "Isolated/Non-Isolated Quad-Inverter Configuration For Multilevel Symmetrical/ Asymmetrical Dual Six-Phase Star-Winding Converter", Conf. Proc., 25th IEEE International Symposium on Industrial Electronics, IEEE-ISIE'16, Santa Clara, CA, (USA), 8–10 Jun. 2016.

978-1-4673-8586-2/16/$31.00 ©2016 IEEE